The influence of milling induced residual stress on fatigue life of aluminum alloys

Luke Berry [a], Greg Wheatley [a,*], Wenchen Ma [b], Reza Masoudi Nejad [c], Filippo Berto [d]

[a] College of Science and Engineering, James Cook University, Townsville QLD 4811, Australia
[b] Phasor Engineering, LLC, 603 S. Main St, Ste 130, Winter Garden, FL 34787, USA
[c] School of Mechanical and Electrical Engineering, University of Electronic Science and Technology of China, Chengdu, 611731, China
[d] Department of Mechanical and Industrial Engineering, NTNU – Norwegian University of Science and Technology, Trondheim, Norway

ABSTRACT

The effect of machining strategies on the surface integrity have received minimal consideration as this fluid situation develops, specifically, the machining induced residual stress generated in the material during milling. This study investigates the presence of machining induced residual stress in Aluminum 7075 and its effects on fatigue life. The testing consists of a layer removal process to measure residual stress followed by a three-point bending fatigue test. The study finds that an increase in feed per tooth in combination with a reduction in cutting speed increases compressive residual stress at the surface in the material. The fatigue testing concludes that this increase in compressive stress improves fatigue life with varying effects on long crack and short crack propagation.

1. Introduction

The influence of the manufacturing processes on material properties has gone unnoticed during recent decades particularly in high-risk industries such as automotive, aviation, and aerospace [1–5]. Sectioning, hole drilling, slotting, and contour methods are the most well-known and common destructive testing methods for residual stress measurements [6]. All these methods and other variations rely on the same concept, the distortion of the component when the cut is induced. Wheatley and Ohta [7] used an adaption of a destructive testing method. In their proposed method, the residual stress was induced by welding and then released through the layer removal method which involved making several fine cuts to allow any residual stress to release. The deformation created by the release of the residual stress is received by strain gauges located on the opposing surface.

Milling is just one of the many ways residual stress occurs in a material with other processes like welding, casting and heat treatment also exhibiting the capability to create locked in stresses (residual stress) [8, 9]. In technical terms, residual stress is generated when the material is loaded beyond its elastic limit causing the stresses to remain after the external loading is removed [10–12]. Milling is susceptible to stress generation from all three mechanisms however research has shown that

the mechanical loading placed on the test piece is by far the most substantial stress influencing the alloy during machining. Zhang et al. [13] investigated the effects of fire-induced high temperatures on the residual punching shear strength of reinforced concrete flat-plate structures after cooling and to examine the effectiveness of a detailing approach for enhancing the post-punching load-carrying capacity. Gao [14] conducted an exclusive study on the effect of initial residual stress on the deformation of thin-walled aluminum components during machining. Wang [15] employed both the layer removal method and a variation of this method referred to as slope cutting in pre-stressed aluminum parts with both initial and machining induced residual stresses. A numerical study conducted by Huang [16] found a relationship between table feed rate (V) and the residual stress. He found that as V increased so did the maximum stress value. Wu et al. [17] studied effects of surface quality and residual stress distribution via x-ray diffraction technique and elastic-viscoplastic FEM. Wyatt et al. [18] concluded that compressive residual stress is generated from the tool piece (mechanical loading) while tensile residual stress is introduced from thermal loadings. Compressive stress at the surface is preferable and in fact can increase component life as it reduces working tensile stress and discourages crack nucleation. Tian [19] implemented a sensitivity analysis on the residual stress in two individual directions: x – parallel to the cut and y

---

* Corresponding author.

Table 1
Mechanical properties and chemical composition of the Aluminum test specimens.

Mechanical properties	Tensile strength (MPa) 599		Yield strength(0.2% offset - MPa) 551			Elongation (%) 10			
Chemical composition (%)	Al Base	Si 0.4	Fe 0.5	Cu 1.2–2	Mn 0.3	Mg 2.1–2.9	Cr 0.18–0.28	Zn 5.1–6.1	Ti 0.2	Other 0.15

(a)

(b)

Fig. 1. aluminum Bar test specimen for (a) residual stress measurements and (b) fatigue life experiments.

Table 2
Machining Parameters for Residual Stress Measurement.

Parameter	Unit	Case 1	Case 2	Case 3	Layer Removal
Cutting speed (Vc)	m/min	251.00	375.00	500.00	132.00
Feed Rate (Vf)	mm/ min	1498.05	1865.10	1989.44	250.00
Spindle speed (n)	rpm	4993.49	7460.39	9947.18	840.34
Feed per Tooth (Fz)	mm	0.08	0.06	0.05	0.07
Feed per revolution (Fn)	mm/ rev	0.3	0.25	0.20	0.30
Tool Diameter (D)	mm	16.00	16.00	16.00	50.00
Number of Flutes (Zn)		4.00	4.00	4.00	4.00
Cutting Width (W)	mm	11.00	11.00	11.00	50.00
Coolant	Yes/No	Yes	Yes	Yes	Yes

Fig. 2. Residual stress measurement apparatus.

–perpendicular to the cut. This favourable behavior was further verified by another study conducted on carbon steel [20]. At a given point in the milling run the residual stress in the feed direction (x-direction) was found to be 912 MPa while the perpendicular direction was found to be 570.08 MPa. Similarly, Rao and Shin [21] conducted a study on the high-speed face milling on Al7075. They reported that the induced machining residual stress was very shallow with the maximum residual stress always being within 40micron from the surface. Historically fatigue life has been broken down into three phases: crack initiation, crack

Fig. 3. The experimental test set-up.

growth and fracture [22,23]. The crack growth phase can be broken into two more distinct phases: small crack and long crack propagation. Lei Zhu [24] understood this field of research was lacking and conducted work on the study of small crack growth behavior with particular attention being given to the machining induced residual stress. Suresh et al. [25] defined the "small crack effect" which describes the differing crack growth rate at the same stress intensity factor. This difference is often higher than that of long crack characteristic which is often utilised to predict fatigue life. Thus, the differing crack growth rate can cause failure to occur before prediction. Other research also found that most of the fatigue life is spent within this erratic small crack fatigue [26–29].

Due to the lack of available research articles on the influence of machining induced residual stress parallels can be drawn between other modes of residual stress such as shot peening. Shot peening is a cold working process that creates severe plastic deformation and can be applied to steels, stainless steels and aluminum [30–32]. In doing so it creates large volumes of residual stress at the surface similar to that of the machining induced residual stress. Cerny et al. [33] verified Benedetti results by also concluding an increase fatigue life on Al-7075 alloy of up to 2.5 times of the un-peened specimen and also concluded that more severe peening has a lesser effect on fatigue life. Gao et al. [34] conducted research into the effect that surface enhancement had on bending fatigue. They agreed that sub surface cracks increased when a compressive residual stress was present on the surface, however they could only assume that this was caused by the enhanced yield strength created at the surface. Other research agreed that crack initiation was common at the sub-surface when surface enhancement (compressive residual stress) was applied however the fatigue life was still improved by 36% [35]. Salvati et al. investigated crack closure and found that if there were a single overloaded cycle it caused the crack growth rate to retard and in the case of an overload/cyclic ratio of 0.7, there was a

complete arrest of the crack growth before re-nucleation of the crack [36]. Colombo et al. [37] supports previous work done by Salvati by doing a direct comparison between cyclic loading and cyclic loading with a single overloaded cycle. Tsukud et al. and Korsunsky et al. also conducted similar research to find the same results with Tsukud detailing that the compressive residual stress was prominent at higher overload ratios [38]. Smith generated promising results by studying effects of residual stress on fatigue life for 52,100 hard turned steel. Smith stated that the hard-tuned specimen had a fatigue life over 56 000 cycles in comparison to a ground surface that was 27 360 cycles, he elaborated by stating the worst hard tuned fatigue test of 16 000 cycles still exceeded the average fatigue life of the grounded surface once outliers were excluded [39]. Moussaoui conducted a comparison between an industry standard for machining and what he considered to be optimal machining conditions with Vc = 50 m/min, d = 0.5 mm and Vc = 32 m/min, d = 3.5 mm. Conversely Javidi et al. found that the stress became more compressive as feed rate increased but noticed variations in fatigue life based on the nose radius used on the tool [40].

There has been little research exploring the relationship between machining induced residual stress and fatigue behavior amongst literature, leaving a vast area unchartered on this topic. In addition, the influence of the milling induced residual stress on fatigue life of Aluminum alloys has not been investigated yet. The focus of this study is to constitute a definitive relation between residual stress profiles generated by milling and resultant effects on fatigue life. The process included two individual testing steps. First, the accurate measurement of residual stress using layer removal. second, an indicative experimental fatigue life using a three-point bending test.

2. Materials and methods

As extruded Al-7075-T6511 bar (50 × 25 × 400 mm^3) was selected as the test piece. This material has been well justified amongst literature as one the most common aircraft grade aluminum's that is at the center of the fatigue failure issue being seen amongst various industries [41]. Mechanical properties and chemical composition of the tested specimens are provided in Table 1 Table 1.

The test piece was cut to a pre-specified length using a band saw. During the experiments, each specimen was fastened to 95 N.m to improve consistency and reduce error. The clamping force created by the stud and nut arrangement is negligible for both the residual stress and the fatigue life measurements. It was assumed that the layer removal did not induce residual stress on the material. Fig. 1-a visualizes the specimen used for the residual stress test. A similar specimen as shown in (a)

Figure Fig. 1-b was manufactured for the fatigue testing. However, the machining of the top surface differs by machining the entire surface to the appropriate parameters detailed in Table 2. The strain gauges were centered in the longest direction and evenly spaced in the shorter direction. Fig. 1 illustrates where the 55 mm and 50 mm cuts will be made down the center of the material.

The residual stress measurement investigates three different machining scenario's spanning from a high-speed machining case to a conventional machining case, as well as considering a non-machined case. Fig. 2 illustrates the Residual stress measurement apparatus. The machining parameters are detailed in Table 2 as well as the machining parameters required for the layer removal process.
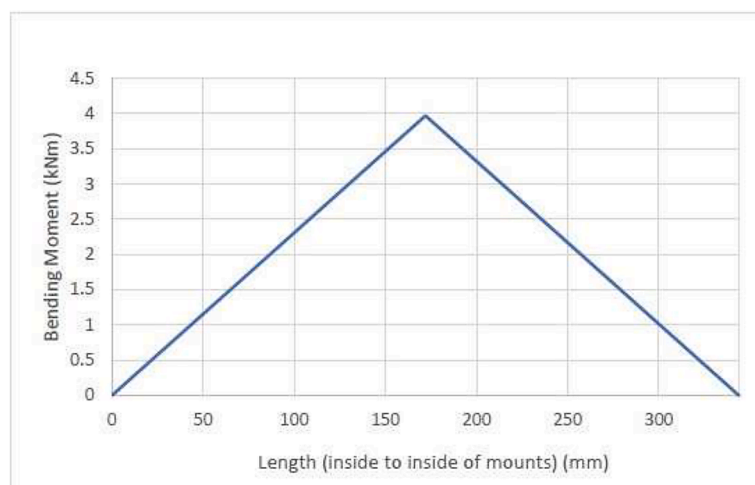
All cuts were made across the material rather than length ways down the material. The machining procedure starts by selecting the Case 1 machining parameters that comprises of a low cutting speed and a high feed per tooth/revolution. These two parameters are some of the most indicative of residual stress highlighted in literature and form the
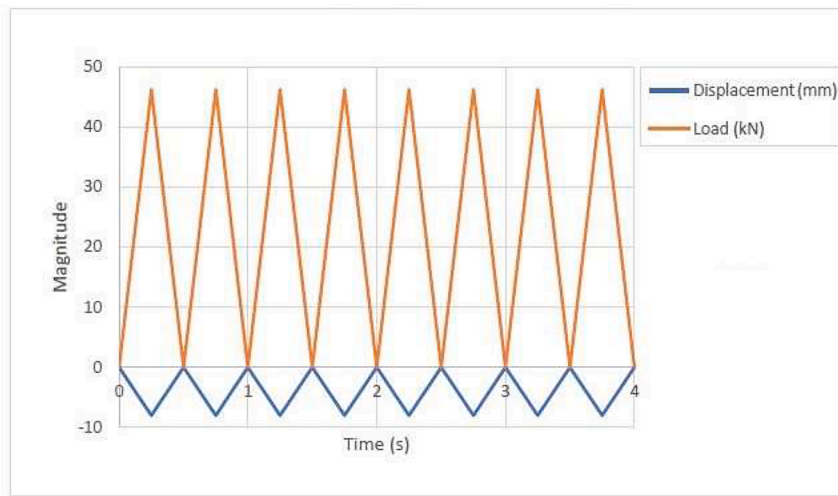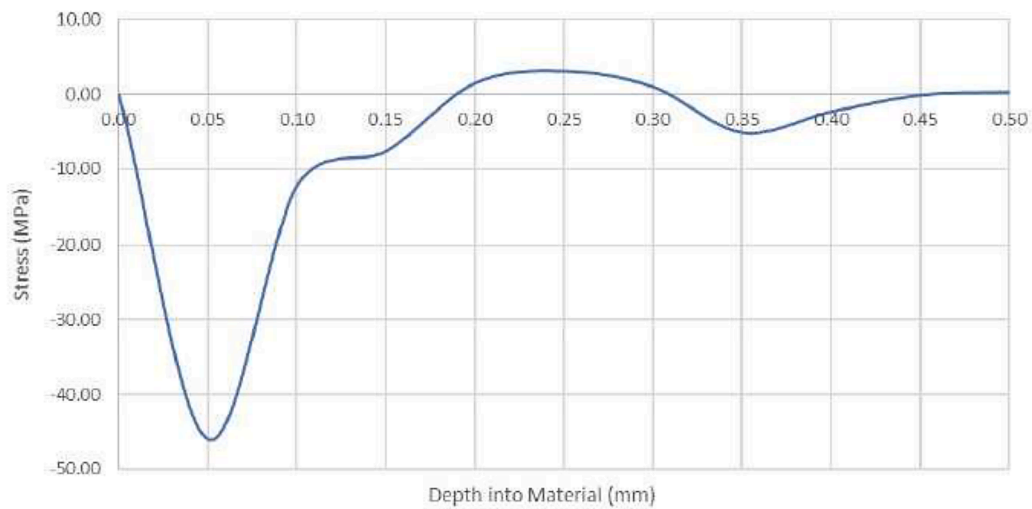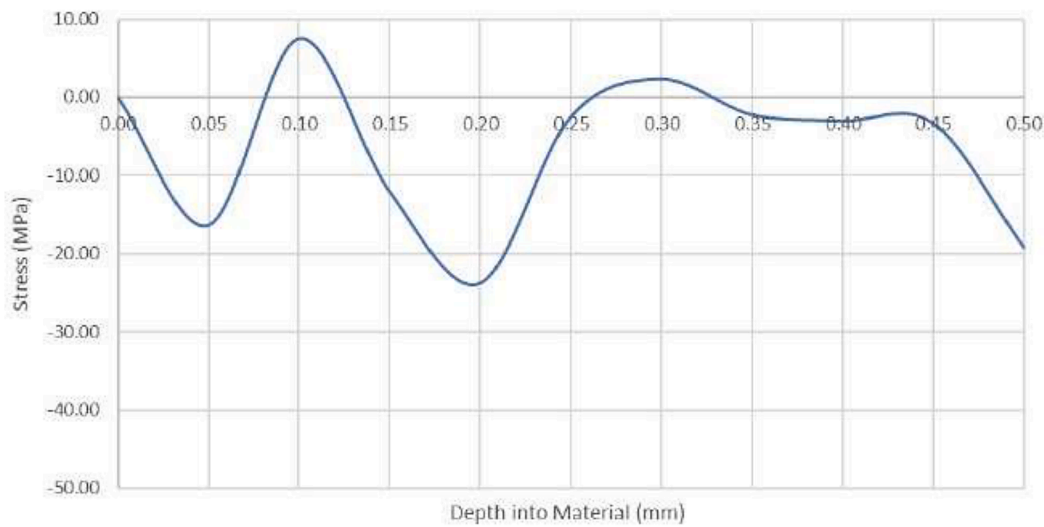
(a)
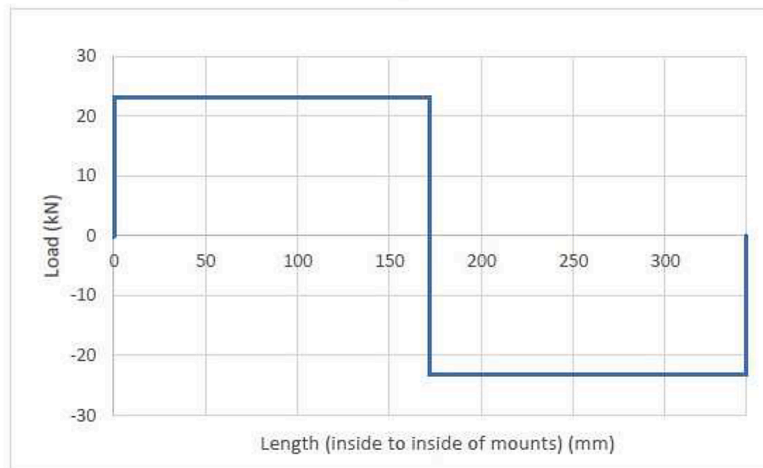
(b)

(c)

Fig. 4. The testing apparatus; (a) Displacement and load pattern, (b) Force diagram, and (c) Bending moment diagram for three-point fatigue testing.

(a)

(b)

Fig. 5. Residual stress induced by machining as per (a) Case1, (b) Case2, (c) Case3, and residual stress in (d) un-machined case.

foundation of this procedure. The corresponding feeds and speeds are consequential of the cutting speed and feed per tooth which were calculated using Equations 1 −3. For Case 1, these magnitudes of cutting speed (251 m/min) and feed per tooth/revolution (0.08 mm and 0.30 mm) were intended to induce the highest residual stress on the material and were passed over the material several times to produce a 55 mm wide pocket at depth of 1 mm. The tooling was then changed to a 50 mm end mill and at this point the FLAB-5–23–1LJC-F strain gauges on the opposing surface were recognized and the data was logged for the following cuts. The successive cuts were ran using the parameters defined in the layer removal column with the intent of only removing the residual stress generated from the Case 1 cut. This was ensured by aligning the parameters with work done by Wang who conducted layer removal on 7075-T651 rolled plate. This method was employed to

determine the residual stress generated within 500 μm of the surface. 500 μm has been identified in literature as the maximum influencing depth of machining with some research indicating even lesser influencing profiles [42]. To achieve the 500 μm depth several cuts were made at a depth of 50 μm and repeated to effectively cover the entire depth of the residual stress profile. A strain measurement was taken between each cut. Later this strain measurement was used to determine stress within the material by applying the stress strain relation used by Wheatley [7]. Once completed the same procedure was carried out for cases 2 and 3 as well as an additional case that does not receive any induced stress but only layer removal.

Another important consideration that was made during the residual stress test was levelness of material. This follows the complex design of the test jig that was manufactured with the dual purpose of allowing the
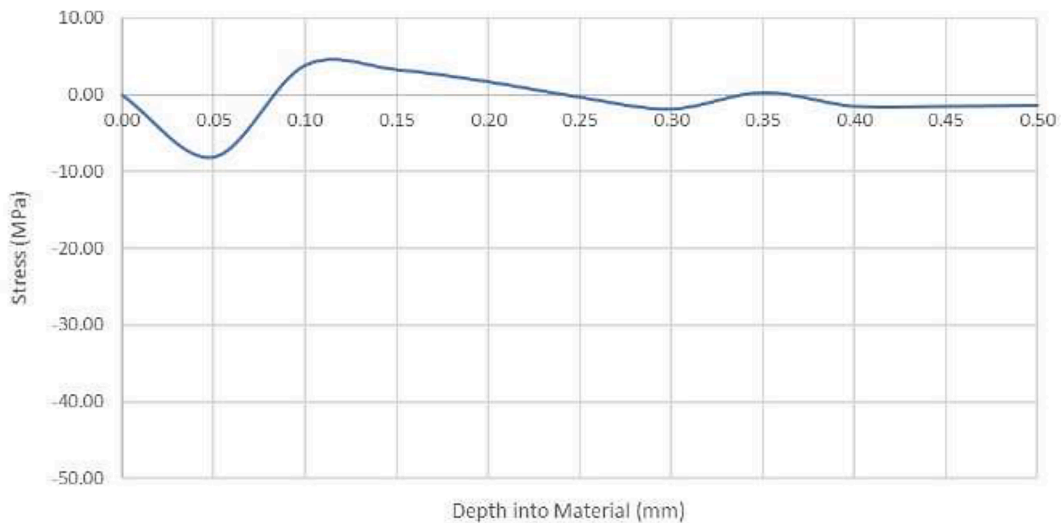
(c)
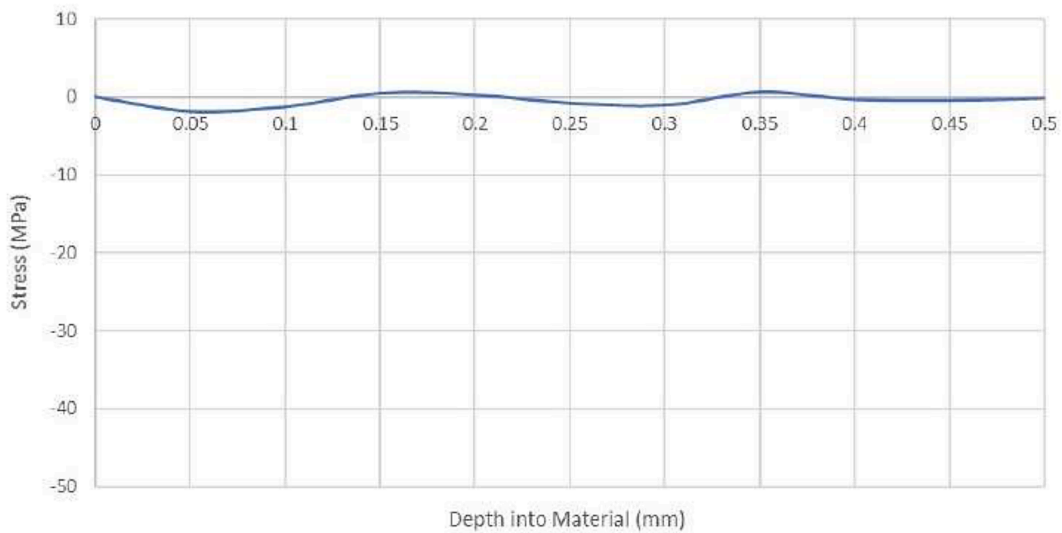
(d)

Fig. 5. (*continued*).

Table 3
The magnitude of the surface residual stress in machining cases.

Machining case	Compressive surface residual stress (MPa)
Case 1	45.95
Case 2	16.33
Case 3	8.14
Un-Machined	1.82

material to deflect without fouling or causing damage to the strain gauges. However, it makes the material susceptible to being out of plane. This resulted in an extra precaution being taken prior to any cuts being made meaning the levelness of the test piece was checked with a tolerance of 0.05 mm across the entire 400 mm length being set. The fatigue life was assessed via a three-point bending test on a hydraulic load frame. The test piece was set up in the jig to allow ease of fitment to the Instron 1342 servo hydraulic UID controlled machine (Fig. 2). The machine has the capability to apply cyclic loads within the range of 15

Hz up to 100 kN. However, the material will receive a fluctuating zero based cyclic load at 2 Hz given the concerns around machine accuracy. Fig. 3-a visualizes a displacement controlled test at a set point of 8 mm. The 8 mm displacement equates to an approximate 46.2 kN dynamic load and 3.97 kN.m at the first cycle (Fig. 3-b and Fig. 3-c). Naturally this load decreases as the material degrades from the service. Pretesting was required to ensure the frame, specimen, and load were appropriate to cycle till failure efficiently and effectively. This was inclusive of trialing different spacers, displacement amplitudes and frequencies. The load frame was calibrated between each test and safety limits were armed at 8.5 mm of displacement and 60 kN of force. Further efforts were made by closely monitoring the specimen and machine readout to reduce possibility of machine error. The loading was cycled till the failure of the test piece. An exception was made for the un-machined case where the material was placed machine side up to eliminate any possible effects of the machining. The experiment was repeated three times for each case, making for a total of 12 tests with every test being logged in the form of displacement-load data. The testing apparatus is shown in Fig. 4, each specimen was run until complete failure.
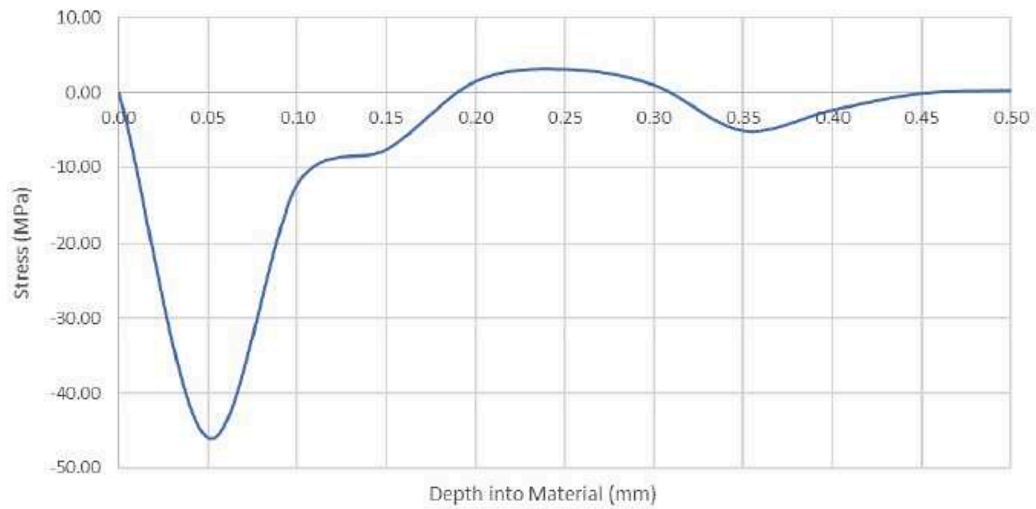
(a)
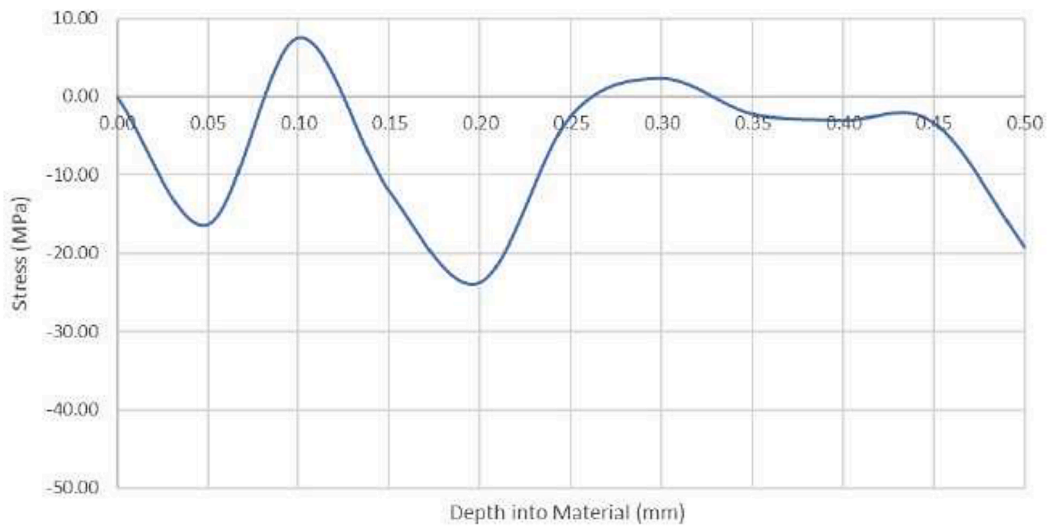
(b)

Fig. 6. Relation of Induced residual stress to fatigue life (cycles) in machined and un-machined test specimens.

3. Results and discussion

3.1. Milling induced residual stress

The strain was continuously recorded by the strain gauges therefore required extensive screening to obtain the most correct result. The strain gauges typically showed a randomized result with multiple peaks and settle points. Screening was critical to obtaining the settled point to be recorded. This data was used to develop the corresponding stress distribution at each layer removal cut using Equitation 4. The residual stress profiles are shown in Fig. 5 which correspond to the Case 1, Case 2, Case 3, and Un-machined case, respectively.

Figure, all residual stress profiles for machined cases conformed well to the proposed residual stress profile identified in the literature [11]. The generated profiles show a large compressive stress at the surface occurring within 0.05 mm in all three cases, followed by a subsurface balancing tensile layer. This tensile layer is induced the outer compressive layer to counter the cutting tool load. With this considered it is obvious that the case 1 exhibited the largest mechanical load, followed by the case 2 and the case 3. The magnitude of the surface residual stress in each case is summarized in Table 3. The table details the reduction in compressive residual surface stress from 46 to16 and then to 8 MPa for Case 1 to Case 3, respectively. This is while cutting speed increases from 251 to 375 to 500 m/min and feed per revolution
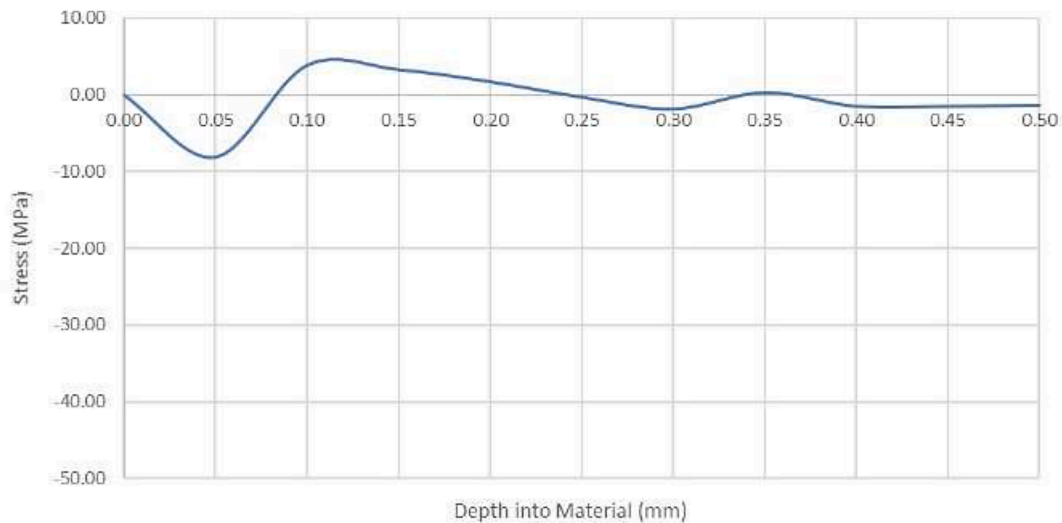
(c)
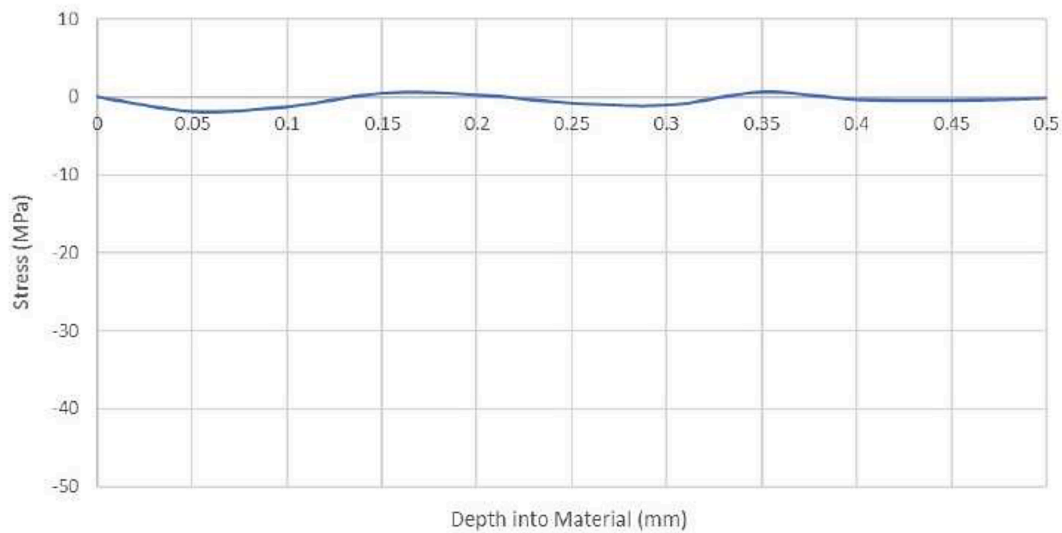
(d)

Fig. 6. (*continued*).

decreases from 0.3 to 0.25 to 0.2 mm/rev. This notable pattern between cases aligns with the trends identified by Wu who proposed that an increase in cutting speed would reduce residual stress while an increase in feed per tooth would increase the residual stress [17]. Machining parameters used in Case 1 were similar to work conducted by Wang [15]. The results of Wang's roughing cut revealed surface residual stress of over 120 MPa at approximately 0.05 mm deep into the material. Both Case 1 and Wang's project used cutting speeds of 251 m/min, a feed rate of 1500 mm/min, a width of cut of 11 mm and a depth of cut of 1 mm. However, surface residual stress reported by Wang was over 120 MPa at approximately 0.05 mm deep into the material which is remarkably different form the residual stress measured in the Case1 (~46 MPa) at the same location. A difference of over 74 MPa is exhibited when compared to residual stress outlined in Table 3. Further investigation shows that Wang's work implemented a 2 flute 16 mm cutter while case

1 used a 4 flute 16 mm cutter. As these two scenarios are both conducted at the same cutting speed and feed rate it would mean that case 1 would see a reduced feed per tooth. This comparison proves that by increasing feed per tooth, residual stress within the material is increased. In addition, this can be closely compared to Wu's work as an increase in feed per revolution allied with an increase in feed per tooth [17]. Thus, the results found in this residual stress measurement proves that an increase in feed per tooth increases residual stress.

3.2. Fatigue life

Fatigue life analysis was carried out on the three machining cases and the non-machined case identified in Table 2. Three-point bending fatigue test was iterated three times in each case to ensure the reliability of the results. The relation between maximum residual stress at the
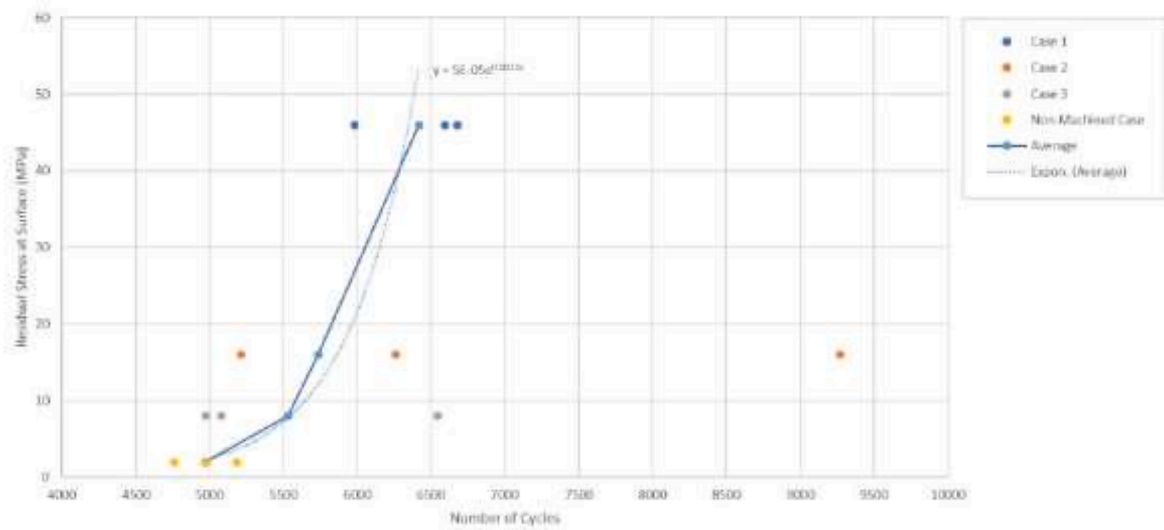
Fig. 6. (*continued*).

(a)

(b)

Fig. 7. Microscopic image of typical fatigue failure of (a) machined and (b) un-machined specimen.

surface and the fatigue life is depicted in Fig. 6.

Fig. 6 concludes that an increase in surface residual stress corresponds to an increase in fatigue life. However, an anomaly was seen in case 2 where the residual stress was 16.33 MPa with a fatigue life of 9272 cycles. This can be attributed to the fact that the material was affected by another surface integrity factor or there was a fault in the testing apparatus, hence why this point was excluded from the average trend. Maximum residual stress was found to have significant influence on the fatigue life. The average of maximum residual stresses achieved at

iterations for each case was taken and it was found fatigue life-residual stress relation could be closely approximated to an exponential formula described by $y = 5E\text{-}05e^{0.0022x}$. Fig. 7 demonstrate the failure surface for the machined and un-machined cases. Noticeably the machined specimens initiate cracks from the corner of the specimen while the un-machined specimen initiates cracks from center of the bottom surface. This behavior was consistent across all specimens. It is proposed that the compressive residual stress generated in the surface relocates the crack initiation sites from the center of the material to the corners. This occurs

Table 4
Long crack fatigue and initiation/short crack fatigue cycles.

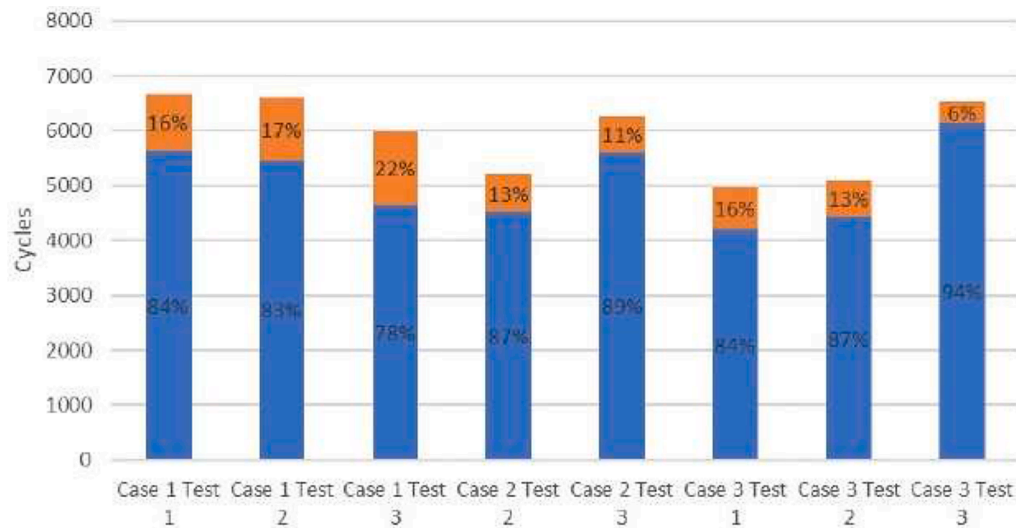|		Case 1 (Cycles)	Case 2 (Cycles)	Case 3 (Cycles)
Test 1	Initiation/Short Crack Fatigue	5624	–	4197
	Long Crack Fatigue	1054	9272	778
Test 2	Initiation/Short Crack Fatigue	5458	4514	4430
	Long Crack Fatigue	1136	702	652
Test 3	Initiation/Short Crack Fatigue	4642	5601	6135
	Long Crack Fatigue	1342	658	408

Fig. 8. Ratio of long crack fatigue and short crack fatigue/initiation.

due to the surface gaining an improved fatigue life causing the crack to initiate from the side of the material near the lower surface.

Table 4 differentiates between long crack and short crack initiation/propagation. This was determined visually where any identifiable crack that was over 500 μm in length was considered as a long crack. The number of cycles before long crack identification was assumed to be either short crack propagation or initiation. This is a common trouble amongst literature where initiation and short crack propagation are difficult to distinguish between. Fig. 8 details the percentage of long crack and short crack propagation/initiation for each case. A common trend of an increase in ratio of short crack propagation to long crack propagation within a given case is seen in Fig. 8. Specifically, in case 1 the short crack propagation increases from 78% to 83% to 84% as the magnitude of cycles increases between each test. In Case 2, short crack propagation increases from 87% to 89% between tests. A similar trend was seen in Case 3 where the short crack propagation increases from 84% to 87% and to 94% between tests. This trend is specific to an increase in number of overall cycles within the chosen machining scenarios. Given that the behavior occurs within a single case it is unlikely that this due to residual stress. Other surface integrity factors could be suggested as the cause of this trend with surface finish and microstructure being considered. The only likely cause for an alteration in surface finish would be tool wear however the effects of tool wear on surface roughness is unclear. Fig. 9 illustrate the individual trends of the short crack fatigue and the long crack fatigue against the surface residual stress, respectively. It should be noted that the un-machined case was excluded from the results since the cracks propagated from the bottom surface could not be identified. The individual results for short crack fatigue do not show any obvious relation to surface residual stress however when the average fatigue life is assessed there is a slight

increase in fatigue cycles of 321 cycles between case 1 and case 3. This shows some signs of retardation of small crack propagation due to the increased surface strength within 0.5 mm of the surface. Contrary to this there is a noticeable increase in Fig. 9-b that suggests surface residual stress increases fatigue life for long crack propagation. Between Case 3 and Case 1. The average number of cycles increases by 565 cycles which is over double the long crack fatigue of case 3. This phenomenon is not consistent with literature that tends to see an increase in short crack fatigue in the presence of compressive surface residual stress. It is suggested that despite statements made in literature residual stress can improve long crack fatigue but may be dependent on geometry. This suggestion stems from the idea that the crack initiates on the edges/sides of the machined surface where the residual stress would have minimal impact on these areas. But the crack is required to propagate across the bottom surface that exhibits large compressive stress thus slowing the long crack propagation across the surface.

4. Conclusions

This main focus of the present study is investigating the influence of manufacturing processes on the fatigue life of aluminum alloys in high-risk applications. In particular, milling of Al7075 alloy was studied with substantial consideration being made from literature regarding the influencing of machining parameters and the effects the corresponding residual stress has on the fatigue life. This was determined by conducting a residual stress measurement of the induced residual stress from three different machining cases as well as considering an un-machined case. This was done by utilizing the layer removal method that has been widely used amongst literature. Next a three-point bending fatigue test was carried out to determine the fatigue life and
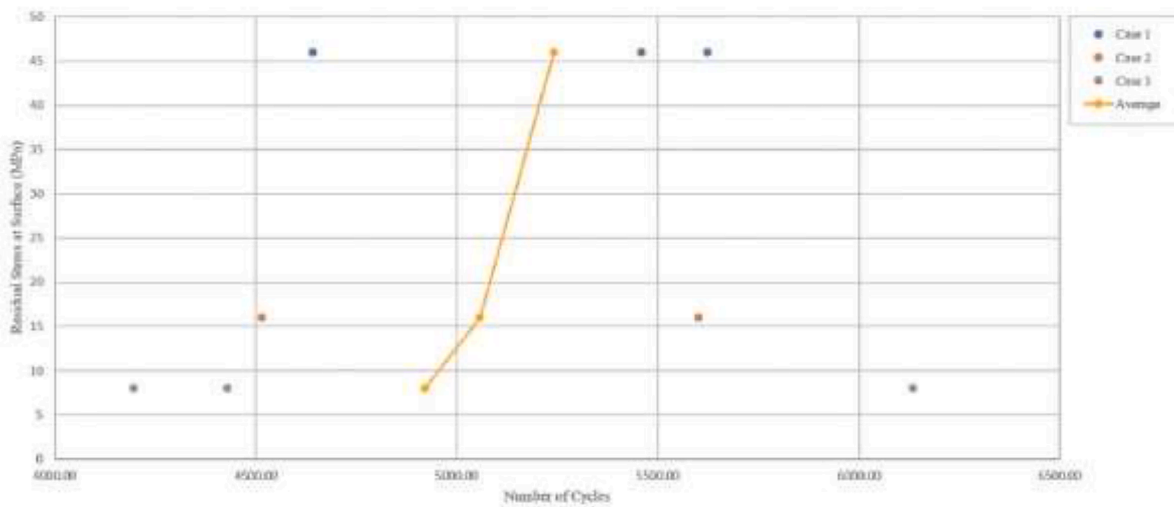
(a)
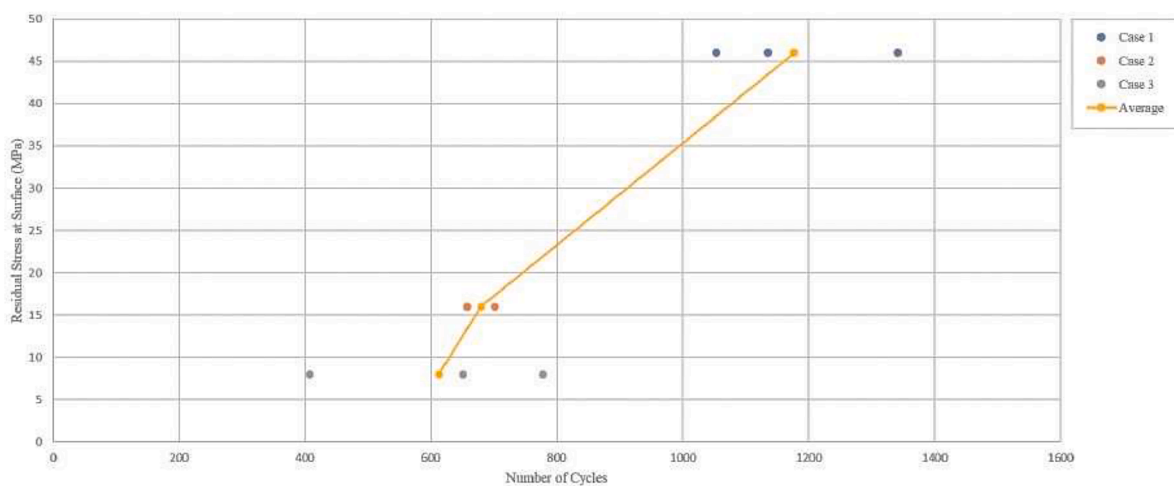
(b)

Fig. 9. Residual stress in relation to (a) short crack fatigue, and (b) long crack fatigue.

its correspondence to the induced residual stress in the material. Once the relevant result interpretation was complete the following conclusions were made:

- By increased the cutting speed reduces surface residual stress in a material while increased feed per tooth increases surface residual stress. Also, machining induced residual stress improves fatigue life in the low cycle regime and can be approximated to an exponential relation.
- Machining induced residual stress is more influential on long crack propagation than short crack propagation/initiation.
- Compressive residual stress on the surface can relocate the crack initiation to a site that is un-machined if the new site is under greater stress than the summation of the loading and residuals stress at the original site.

Declaration of Competing Interest

The authors declare that they have no known competing financial interests or personal relationships that could have appeared to influence the work reported in this paper.

References

[1] Behnam Niknam, Farhad Haji Aboutalebi, Wenchen Ma, Reza Masoudi Nejad, Effect of variations internal pressure on cracking radiant coils distortion, Structures 34 (2021) 4986–4998.
[2] Wanhai Xu, Yuhan Li, Wenchen Ma, Kai Liang, Yang Yu, Effects of spacing ratio on the FIV fatigue damage characteristics of a pair of tandem flexible cylinders, Appl. Ocean Res. 102 (2020), 102299.
[3] Wan-hai Xu, Qian-nan Zhang, Wen-chen Ma, En-hao Wang, Response of two unequal-diameter flexible cylinders in a side-by-side arrangement: characteristics of FIV, China Ocean Eng. 34 (4) (2020) 475–487.
[4] Reza Nejad, Mohammadreza Tohidi, Ahmad Jalayerian Darbandi, Amin Saber, Mahmoud Shariati, Experimental and numerical investigation of fatigue crack growth behavior and optimizing fatigue life of riveted joints in Al-alloy 2024 plates, Theor. Appl. Fract. Mech. 108 (2020), 102669.
[5] Mahmoud Shariati, Majid Mirzaei, Reza Masoudi Nejad, An applied method for fatigue life assessment of engineering components using rigid-insert crack closure model, Eng. Fract. Mech. 204 (2018) 421–433.
[6] Reza Masoudi Nejad, Zhiliang Liu, Wenchen Ma, Filippo Berto, Reliability analysis of fatigue crack growth for rail steel under variable amplitude service loading conditions and wear, Int. J. Fatigue 152 (2021), 106450.
[7] G. Wheatley, A. Ohta, On Fatigue Life Improvement Using Low Transformation Temperature Weld Material, Structural Integrity and Fracture, 2002, pp. 201–205.

[8] C. Autodesk, Fundamentals of CNC Machining, Titans of CNC, 2014.

[9] G.S. Schajer, Practical Residual Stress Measurement Methods, John Wiley & Sons, 2013.

[10] Reza. Masoudi, Numerical study on rolling contact fatigue in rail steel under the influence of periodic overload, Eng. Fail. Anal. 115 (2020), 104624.

[11] Reza Masoudi Nejad, Zhiliang Liu, Wenchen Ma, Filippo Berto, Fatigue reliability assessment of a pearlitic Grade 900A rail steel subjected to multiple cracks, Eng. Fail. Anal. 128 (2021), 105625.

[12] Reza Masoudi Nejad, The effects of periodic overloads on fatigue crack growth in a pearlitic Grade 900A steel used in railway applications, Eng. Fail. Anal. 115 (2020), 104687.

[13] Chunyu Zhang, Wenchen Ma, Xiang Liu, Ying Tian, Sarah L. Orton, Effects of high temperature on residual punching strength of slab-column connections after cooling and enhanced post-punching load resistance, Eng. Struct. 199 (2019), 109580.

[14] H. Gao, et al., Investigation on influences of initial residual stress on thin-walled part machining deformation based on a semi-analytical model, J. Mater. Process. Technol. 262 (2018) 437–448.

[15] Z. Wang, et al., An analytical model to predict the machining deformation of frame parts caused by residual stress, J. Mater. Process. Technol. 274 (2019), 116282.

[16] K. Huang, W. Yang, X. Ye, Adjustment of machining-induced residual stress based on parameter inversion, Int. J. Mech. Sci. 135 (2018) 43–52.

[17] Q. Wu, D.-.P. Li, Analysis and X-ray measurements of cutting residual stresses in 7075 aluminum alloy in high speed machining, Int. J. Precis. Eng. Manuf. 15 (8) (2014) 1499–1506.

[18] J. Wyatt, J. Berry, A new technique for the determination of superficial residual stresses associated with machining and other manufacturing processes, J. Mater. Process. Technol. 171 (1) (2006) 132–140.

[19] W. Tian, et al., Sensitivity analysis of the influence of milling parameters on the surface residual stress of titanium alloy TC11, Procedia CIRP 56 (2016) 149–154.

[20] N. Masmiati, A.A. Sarhan, Optimizing cutting parameters in inclined end milling for minimum surface residual stress–Taguchi approach, Measurement 60 (2015) 267–275.

[21] B. Rao, Y.C. Shin, Analysis on high-speed face-milling of 7075-T6 aluminum using carbide and diamond cutters, Int. J. Mach. Tools Manuf 41 (12) (2001) 1763–1781.

[22] Wenchen Ma, Behavior of Aged Reinforced Concrete Columns under High Sustained Concentric and Eccentric Loads. PhD diss., University of Nevada, Las Vegas, 2021.

[23] Wenchen Ma, "Simulate Initiation and Formation of Cracks and Potholes," Master Report, Northeastern University, Boston, Massachusetts, USA, 2016.

[24] L. Zhu, et al., Comparative study of small crack growth behavior between specimens with and without machining-induced residual stress of alloy GH4169, J. Mech. Sci. Technol. 32 (11) (2018) 5251–5261.

[25] S. Suresh, Fatigue of Materials, Cambridge university press, 1998.

[26] Reza Masoudi, Zhiliang Liu, Effect of periodic overloads and spectrum loading on fatigue life and microstructure in a Grade 900A rail steel, Theor. Appl. Fract. Mech. 110 (2020), 102796.

[27] Reza Masoudi Nejad, Zhiliang Liu, Analysis of fatigue crack growth under mixed-mode loading conditions for a pearlitic Grade 900A steel used in railway applications, Eng. Fract. Mech. 247 (2021), 107672.

[28] M. Okazaki, H. Yamada, S. Nohmi, Temperature dependence of the intrinsic small fatigue crack growth behavior in Ni-base superalloys based on measurement of crack closure, Metall. Mater. Trans. A 27 (4) (1996) 1021–1031.

[29] M. Rokni, et al., Microstructure and mechanical properties of cold sprayed 6061 Al in As-sprayed and heat treated condition, Surf. Coat. Technol. 309 (2017) 641–650.

[30] M. Benedetti, et al., Reverse bending fatigue of shot peened 7075-T651 aluminium alloy: the role of residual stress relaxation, Int. J. Fatigue 31 (8–9) (2009) 1225–1236.

[31] O. Unal, R. Varol, Surface severe plastic deformation of AISI 304 via conventional shot peening, severe shot peening and repeening, Appl. Surf. Sci. 351 (2015) 289–295.

[32] A. Bag, et al., Effect of different shot peening conditions on the fatigue life of 300M steel submitted to high stress amplitudes, Int. J. Fatigue 130 (2020), 105274.

[33] I. Černý, J. Sís, D. Mikulova, Short fatigue crack growth in an aircraft Al-alloy of a 7075 type after shot peening, Surf. Coat. Technol. 243 (2014) 20–27.

[34] Y.K. Gao, Bending fatigue strengths/limits of smooth specimens with and without surface-enhanced layer of aeronautical metallic alloys, Int. J. Struct. Integr. (2011).

[35] Y.-k. Gao, et al., Influence of surface integrity on fatigue strength of 40CrNi2Si2MoVA steel, Mater. Lett. 61 (2) (2007) 466–469.

[36] E. Salvati, et al., Separating plasticity-induced closure and residual stress contributions to fatigue crack retardation following an overload, J. Mech. Phys. Solids 98 (2017) 222–235.

[37] C. Colombo, et al., On crack tip shielding due to plasticity-induced closure during an overload, Fatigue Fract. Eng. Mater. Struct. 33 (12) (2010) 766–777.

[38] H. Tsukuda, H. Ogiyama, T. Shiraishi, Fatigue crack growth and closure at high stress ratios, Fatigue Fracture Eng. Mater. Struct. 18 (4) (1995) 503–514.

[39] S. Smith, et al., Effect of surface integrity of hard turned AISI 52100 steel on fatigue performance, Mater. Sci. Eng.: A 459 (1–2) (2007) 337–346.

[40] A. Javidi, U. Rieger, W. Eichlseder, The effect of machining on the surface integrity and fatigue life, Int. J. Fatigue 30 (10–11) (2008) 2050–2055.

[41] R. Bucci, Selecting aluminum alloys to resist failure by fracture mechanisms, Eng. Fract. Mech. 12 (3) (1979) 407–441.

[42] J.-g Li, S.-q. Wang, Distortion caused by residual stresses in machining aeronautical aluminum alloy parts: recent advances, Int. J. Adv. Manuf. Technol. 89 (1–4) (2017) 997–1012.